Available online at www.sciencedirect.com

ScienceDirect

Russian Geology and Geophysics 59 (2018) 690–696

RUSSIAN GEOLOGY AND GEOPHYSICS

www.elsevier.com/locate/rgg

Magnetic viscosity effect on TEM data of an array with a fixed transmitter loop

N.O. Kozhevnikov [a,b,*], E.Yu. Antonov [a]

[a] *A.A. Trofimuk Institute of Petroleum Geology and Geophysics, Siberian Branch of the Russian Academy of Sciences, pr. Akademika Koptyuga 3, Novosibirsk, 630090, Russia*

[b] *Novosibirsk State University, ul. Pirogova 2, Novosibirsk, 630090, Russia*

Received 14 April 2017; accepted 2 August 2017

Abstract

In this paper, we present and discuss the results of modeling of the transient induction processes observed at different distances from the center of a transmitter loop in studies of a two-layer earth in which the magnetic susceptibility of the top layer or the base depends on frequency. Profiling graphs (the offset is plotted on the abscissa, and the EMF induced in the receiver coil at a fixed time is plotted on the ordinate) show that the polarity of the EMF changes as the offset increases. For the model with a magnetic layer of any thickness, the polarity of the EMF reverses immediately after the receiver crosses the loop wire. For the model with a magnetic base, the offset at which the EMF polarity reversal occurs is the larger the greater the thickness of the layer. For both models, the EMF at a fixed time depends on the thickness of the layer and the offset. Particularly strong dependence of the EMF on layer thickness or offset is observed near the loop side. Therefore, measurements near the wire make it possible to determine the thickness of the layer in the case where it is much less than the length of the loop side. The overall effect of magnetic relaxation and transient eddy currents leads to the fact that small changes in the layer thickness or offset can lead to a dramatic change in the transient response.

Keywords: TEM method; magnetic viscosity; two-layer model; fixed source array

Introduction

Magnetic viscosity is one of the fundamental properties of ferromagnetic materials. This effect involves a delay in changes in the magnetic characteristics of ferromagnets with respect to changes in the strength of the external magnetic field. In rocks, magnetic viscosity effects are mainly associated with the magnetization and magnetic relaxation of ultrafine particles of ferrimagnetic minerals—the superparamagnetism phenomenon.

The magnetic relaxation times of superparamagnetic (SPM) particles of ferrimagnetic minerals are 10^{-9} to 10^{2} s or more. This time interval includes the range of recording times of EMF measured in transient electromagnetic method (TEM), so that the magnetic relaxation of superparamagnetic particles affects inductive transient responses.

It is known (Kozhevnikov and Antonov, 2008, 2009) that the resulting signal in the receiver coil can be represented as the sum of the EMFs e_1 and e_2 induced by magnetic relaxation and eddy currents, respectively. The EMF e_1 decreases in inverse proportion to the first power of time t:

$$e_1(t) = bt^{-1}, \tag{1}$$

where b is a time-independent coefficient determined by the array geometry. The EMF e_2 decreases much faster. In particular, for a homogeneous conducting half-space, $e_2(t) \propto t^{-5/2}$. Therefore, the relative contribution of $e_1(t)$ to the total response is steadily increasing over time. At a certain moment, the magnetic relaxation effect becomes predominant. This moment depends on the spatial distribution of the electrical conductivity and the content of SPM particles, as well as on the geometry and dimensions of the transmitter-receiver array.

Accounting for the effect of the magnetic viscosity of geological media on TEM responses is an essential problem in TEM surveys. Mathematical modeling plays an important role in the solution of this problem. Previously, magnetic viscosity effects have been studied mainly for the coaxial loop and one-loop configurations (Kozhevnikov and Antonov, 2008, 2009, 2011). For offset arrays, modeling has been

* Corresponding author.
E-mail address: KozhevnikovNO@ipgg.sbras.ru (N.O. Kozhevnikov)

1068-7971/$ - see front matter © 2018, V.S. Sobolev IGM, Siberian Branch of the RAS. Published by Elsevier B.V. All rights reserved.
http://dx.doi.org/10.1016/j.rgg.2018.05.007

performed in a limited scope for the case where the source and receiver are located on the surface of a homogeneous magnetically viscous half-space (Kozhevnikov and Antonov, 2008).

In this paper, using the two-layer earth model as an example, it is shown how magnetic viscosity effects manifest themselves depending on the model parameters and the array offset defined as the distance r between the centers of the transmitter loop and the receiver coil. As in our previous works, the adjectives "magnetically viscous" and "magnetic" are used as synonyms, as well as the adjectives "nonmagnetically viscous" and "nonmagnetic," to avoid repetition.

Calculation of TEM responses taking into account magnetic viscosity

There are two methods for calculating the TEM responses with magnetic viscosity taken into account (Kozhevnikov and Antonov, 2008, 2009, 2011). The first method is based on the relationship between viscous magnetization and associated magnetic field penetrating the receiver coil. In this case, the calculation is carried out in the time domain using the time-dependent magnetic susceptibility:

$$\kappa(t) = \frac{\Delta\kappa}{\ln(\tau_2/\tau_1)}(B + \ln t),$$

where t is the time after switching on or off the primary magnetic field (time delay); $\Delta\kappa$ is the difference between the static ($t \to \infty$) and dynamic ($t \to 0$) susceptibilities; τ_1 and τ_2 are the lower and upper limits of the range of magnetic relaxation times; B is a constant.

The second method is based on the solving the boundary-value problem of the Helmholtz equation for a source located on the surface of a horizontally-layered conducting magnetically viscous ground. The solution is obtained in the frequency domain and then converted into the time domain. The magnetic viscosity effect is taken into account by using the complex frequency-dependent magnetic susceptibility (Lee, 1984):

$$\kappa(\omega) = \Delta\kappa\left[1 - \frac{1}{\ln(\tau_2/\tau_1)} \cdot \ln\frac{1 + j\omega\tau_2}{1 + j\omega\tau_1}\right],$$

where ω is the circular frequency, $j = \sqrt{-1}$, $\Delta\kappa$ is the difference between the magnetic susceptibilities at low ($\omega \ll 1/\tau_2$) and high ($\omega \gg 1/\tau_1$) frequencies (the magnetic susceptibility decrement).

For the calculations presented and discussed in this paper, the second method was used.

Characteristics of models

Just as a homogeneous half-space plays a fundamental role among the set of geoelectric models, two-layer models occupy a special place among horizontally-layered models (Fig. 1). In this paper, two two-layer models are considered.

Model 1 is represented by a magnetically viscous layer lying on a nonmagnetic base. It describes various geological objects. Often, the surface layer contains a large amount of superparamagnetic particles of ferrimagnetic minerals, whose magnetic relaxation manifests itself as a magnetic viscosity effect. Superparamagnetic particles can initially be present in rocks, e.g., in traps, tuffs, and basalts (Kozhevnikov et al., 2016; Worm and Jackson, 1999; Zakharkin et al., 1988) or can be products of exogenous processes, e.g., weathering (Buselli, 1982; Heller and Evans, 2003) as well as by-products of human or bacterial activity (Colani and Aitken, 1966; Linford, 2005). The thickness of magnetically viscous layers varies from a few or a few tens of centimeters (soil) to hundreds of meters, e.g., in Western Yakutia, where weakly magnetic carbonate rocks are overlain by traps and tuffs.

Model 2 is formed by a nonmagnetic layer overlying a magnetically viscous base. It corresponds to the cases where nonmagnetic rocks overlie layers of basalts, traps, tuffs, and other magnetically-viscous rocks. This model is used in archeogeophysics to study natural and man-made objects of relatively small size, e.g., accumulations of ancient metallurgical slags under modern sediments. For $\rho_1 \to \infty$, the model can be of interest in interpreting airborne TEM data obtained in areas where magnetic viscosity effects are observed (Macnae, 2016).

As previously (Kozhevnikov and Antonov, 2008, 2009, 2011), we assumed in the calculations that $\tau_1 = 10^{-6}$ s and $\tau_2 = 10^6$ s (Kozhevnikov and Antonov, 2008, 2009, 2011). The value of $\Delta\kappa$ was 10^{-2} SI units, which agrees in order of magnitude with the estimates obtained by inversion of TEM responses for tuffs and traps in the Malobotuobinskii region in Western Yakutia (Stognii et al., 2010) and basalts of the Vitim plateau in Transbaikalia (Kozhevnikov and Antonov, 2012).

Array

The calculations presented in this paper were performed for an array with a 25×25 m transmitter loop. This choice is due to the fact that the magnetic viscosity effect on TEM responses is more often observed when using small-size arrays. In this case, even at early times, the TEM signal drops to the noise level, whereas the EMF induced by magnetic relaxation exceeds this level. On the other hand, arrays with a transmitter loop of this or similar size are commonly used in near-surface TEM surveys.

As regards measurements at late (≥ 0.5 s) times, only recently has the quality of such measurements reached a level where "nuances" of transient responses can be reliably identified as magnetic viscosity effects (Kozhevnikov et al., 2016). At the same time, in areas where traps and tuffs are common, magnetic viscosity effects at late times during operation of transmitter loops of large size at offsets above 1 km were observed as early as 30 years ago (Zakharkin et al., 1988).

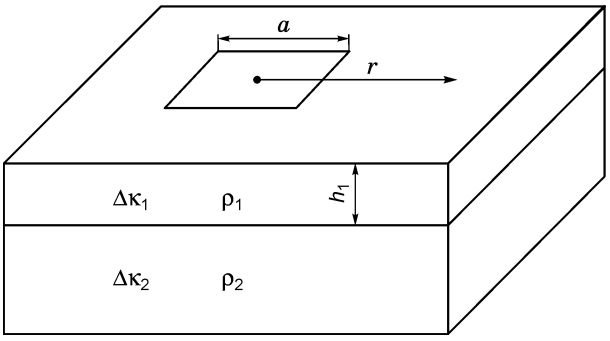

Fig. 1. Transmitter loop on the surface of a two-layer half-space: ρ_1 and ρ_2 are the resistivities and $\Delta\kappa_1$ and $\Delta\kappa_2$ are the magnetic susceptibility decrements of the top layer and the base, respectively, h_1 is the layer thickness, a is the length of the transmitter loop, and r is the transmitter–receiver offset.

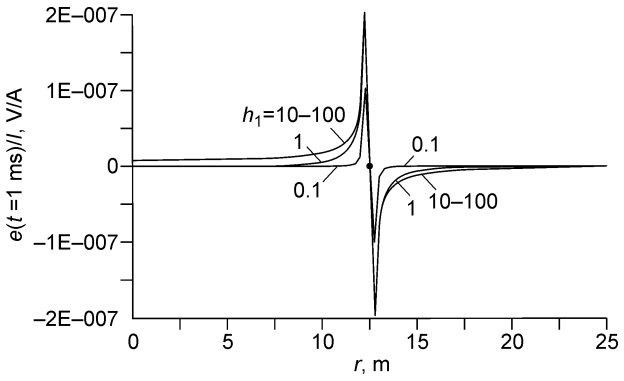

Fig. 2. Graphs of the EMF normalized to the transmitter current versus offset. h_1 is the thickness of the top layer (m). Here and in Figs. 3, 4, and 5, the point at a distance r = 12.5 m indicates the place where the profile crosses the loop wires. The model parameters are $\rho_1 = \rho_2 = 10^6$ Ω·m, $\Delta\kappa_1 = 0.01$ SI units, $\Delta\kappa_2 = 0$, and h_1 = 0.1–100 m.

Calculation results

The modeling of magnetic viscosity effects was carried out in stages. Initially, for both models, the resistivity of the layer (ρ_1) and the base (ρ_2) was assumed to be 10^6 Ω·m. For this high resistivity, eddy currents decay very rapidly, which allowed magnetic viscosity effects to be studied taken alone.

Then, calculations were performed which provided an understanding of how magnetic viscosity manifests itself against the background of the effects produced by eddy currents. In this case, the electrical resistivity of the layer and the base was 100 Ω·m.

Stage 1, model 1. The array was located on the surface of a magnetically viscous layer ($\Delta\kappa_1 = 0.01$ SI units) underlain by a nonmagnetic base ($\Delta\kappa_2 = 0$). The layer thickness h_1 varied from 0.1 to 100 m. In the calculations, it was assumed that the size of the receiver coil was 0.1× 0.1 m and the number of turns was 100 (effective area of 1 m^2). The small size of the loop made it possible to study magnetic viscosity effects near (at a distance of 1 m and less) the wire.

Figure 2 shows graphs of the EMF (normalized to the transmitter current) induced in the receiver coil at time t = 1 ms along the profile which starts at the center of the loop (r = 0), crosses it (r = 12.5 m), and ends outside (r = 25 m).

As can be seen, when the receiver coil is inside the transmitter loop, the EMF first remains almost unchanged with increasing offset, but then, closer to the wire, it increases more and more rapidly. Regardless of the thickness of the layer, the polarity reversal of the EMF occurs beyond the loop (r = 12.5 m). As for the receiver located inside the loop, for its location outside the loop, maximum EMF magnitudes are also observed near the wire. As the receiver coil is moved away from the wire, the EMF decreases in magnitude; furthermore, the rate of change in the EMF as a function of r is the higher the smaller the distance from the loop wire to the receiver coil.

Increasing h_1 leads to a change in the level and shape of the profiling graphs. A particularly strong effect of the layer thickness on the shape of the graphs is observed near the wire. The sensitivity of the EMF to a change in layer thickness is the higher the thinner the layer. For $h_1 > 10$ m, the profiling graphs do not react to further increase in h_1; i.e., the effect of the layer becomes indistinguishable from that observed on the surface of a magnetic half-space.

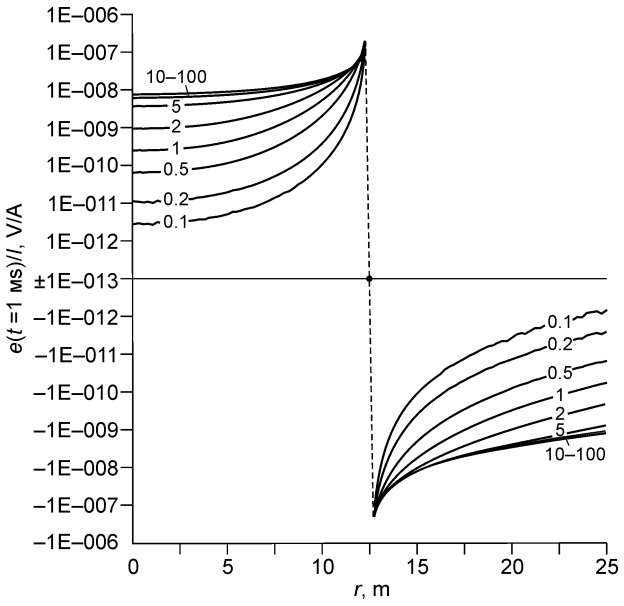

Fig. 3. Graphs of the EMF normalized to the transmitter current (at a time of 1 ms) versus offset on a logarithmic scale. For symbols see Fig. 2.

When the receiver coil is outside the loop, the EMF decreases monotonically and approaches zero as r increases. However, when the loop is moved from the wire to the center of the loop, the EMF approaches a certain positive value, which is the higher the thicker the layer. In the central part of the loop, the EMF and hence the secondary magnetic field do not depend on r.

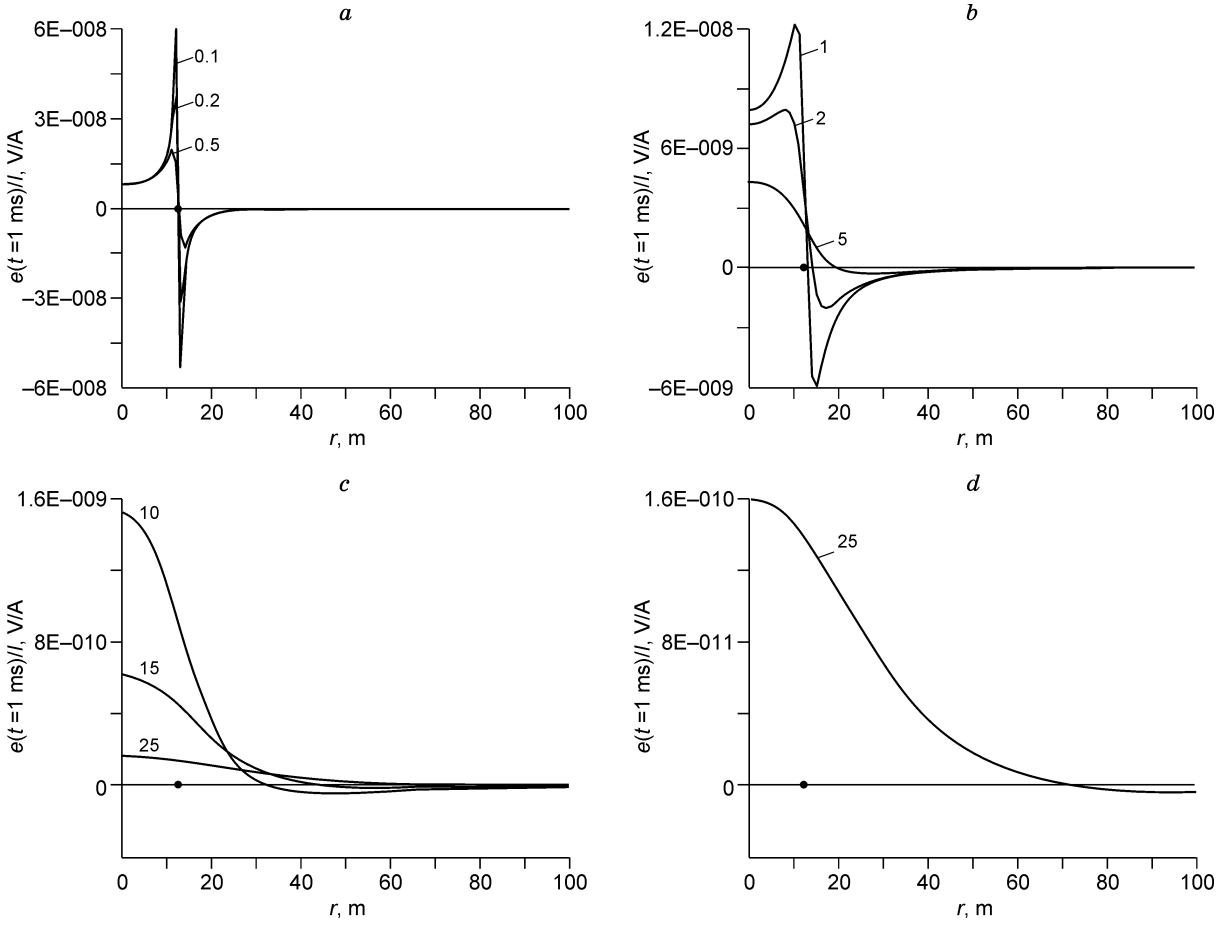

Fig. 4. Graphs of the EMF normalized to the transmitter current (at a time of 1 ms) versus offset. The model parameters are $\rho_1 = \rho_2 = 10^6$ Ω·m, $\Delta\kappa_1 = 0$, $\Delta\kappa_2 = 0.01$ SI units, and $h_1 = 0.1$–25 m (thickness of the top layer). *a*–*d*, For a description, see the text.

Profiling graphs on a logarithmic scale (Fig. 3) display magnetic viscosity effects for the entire range of the layer thickness.

Stage 1, model 2. The array was located on the surface of a nonmagnetic ($\Delta\kappa_1 = 0$) layer underlain by a magnetically viscous base ($\Delta\kappa_2 = 0.01$ SI units). As in the case considered above, the calculations were performed for h_1 in the range of 0.1 to 100 m. The evaluations preceding the main calculations showed that for $h_1 \geq 1$ m, the profiling graphs became smooth and magnetic viscosity effects occurred even at a considerable distance from the source. Therefore, in the main calculations, the length of the profile was 100 m and the observation step was equal to 1 m. EMF was assumed to be measured with a 1×1 m single-turn receiver coil. The results of the calculations are shown in Fig. 4.

When the magnetically viscous base is at a shallow depth, i.e., when $h_1 \ll a$ (Fig. 4*a*), the EMF increases more and more rapidly when at approaching the wire. Polarity reversal of the EMF occurs when the receiver coil falls outside the loop. With further increase in the offset, the EMF decreases in magnitude while remaining negative. The rate of decrease in the EMF is maximal near the wire and decreases away from it. As h_1 increases (Fig. 4*b*, *c*), the graphs become smoother, the maximum inside the loop moves to its center, and the polarity reversal of the EMF occurs at increasingly larger *r*. In Fig. 4*d*, the profiling graph for $h_1 = 25$ m is shown on a large scale, so that it is seen that in this case the EMF polarity reverses at $r = 70$ m.

Stage 2. Recall that due to the high (10^6 Ω·m) resistivity, the above results correspond to the case where the contribution of the magnetic field of eddy currents to the total transient response is negligible compared to the magnetic viscosity effect. For resistivities typical of most rocks, the effect of eddy currents should be taken into account. Below this influence is considered for model 2 as an example.

Figure 5*a* illustrates how the profiling graphs ($t = 1$ ms) change as the resistivity of the layer and the base decreases from 10^6 to 10^2 Ω·m. The profiling graph for the conductive ground is higher than that for the high-resistivity one and its shape also changed. Although the EMF is still a nonmonotonic function of *r*, its polarity within the entire profile remains positive. Figure 5*b* shows profiling graphs for three values of h_1 for the conductive ($\rho_1 = \rho_2 = 10^2$ Ω·m) model.

When the effect of eddy currents can be neglected, there is always a change in the EMF polarity outside the loop

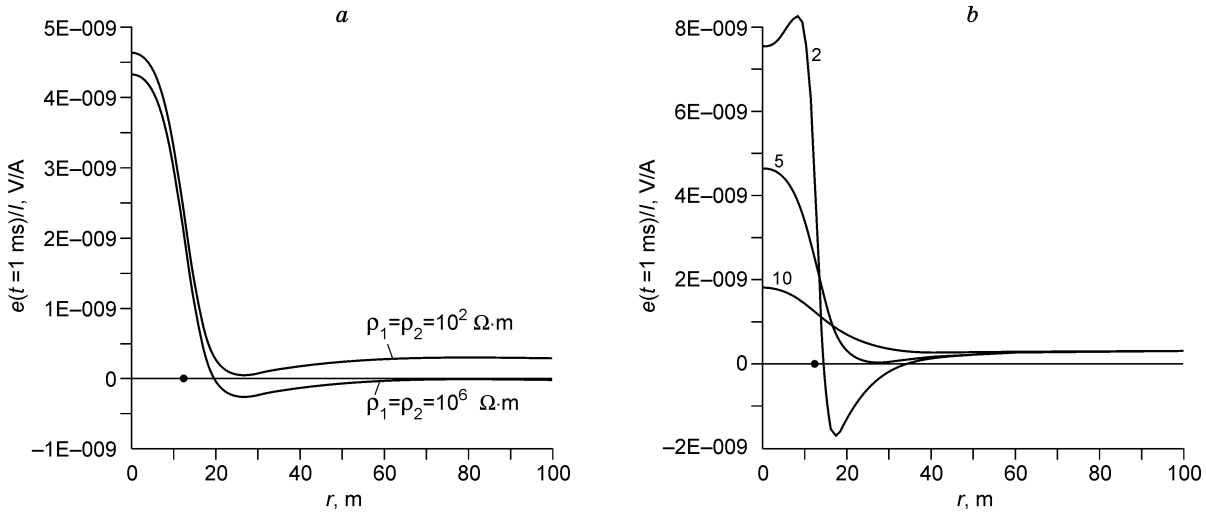

Fig. 5. Effects exerted on profiling graphs by the resistivity of the layer and of the base with unchanged layer thickness (h_1 = 5 m) (*a*) and by the layer thickness (2, 5, 10 m) with unchanged resistivity ($\rho_1 = \rho_2 = 10^2$ Ω·m) of the layer and the base (*b*).

(Fig. 4). If the contribution of eddy currents to the total transient response is significant (Fig. 5*b*), polarity reversal is observed only when the layer thickness is small. As h_1 increases, the EMF becomes positive within the entire profile. For $h_1 \geq 5$ m, the shape of the graphs flattens out and their total level decreases.

In the above consideration of magnetic viscosity effects, the calculation results are presented in the form of profiling graphs at a time delay of 1 ms. In accordance with expression (1), the profiling graphs in Figs. 2–5 are easily recalculated for any time. For example, to construct graphs for $t = 0.1$ ms, the EMF values on the profiling graphs should be multiplied by 10, and for $t = 10$ ms, they should be divided by 10.

The profiling graphs visually illustrate how magnetic viscosity effects vary in space. Obviously, the time dependence of the EMF is of no less interest. Let us consider how the magnetic viscosity effect depends on time using model 2 as an example.

As is known, at late times, the polarity of the EMF e_2 induced in the receiver by eddy currents is positive and does not depend on the offset (McNeill, 1980). Unlike e_2, the EMF e_1 generated by magnetic relaxation becomes negative at a certain distance from the loop wire (Fig. 4). Therefore, if the receiver is located outside the loop at a short distance from the wire, the total EMF is positive and monotonically decreasing in time. As the receiver is moved away from the loop, e_1 becomes negative and the total EMF changes polarity with time (Fig. 6). Furthermore, small changes in the loop position or layer thickness lead to drastic changes in the total transient response.

Discussion of the results

The above results show that for both models, magnetic viscosity effects depend on the thickness of the top layer and the offset. A characteristic feature of the profiling graphs is the sign reversal of the EMF outside the loop. We denote by r_{SR} the offset at which polarity reversal occurs.

For model 1, regardless of the thicknesses of the magnetic layer, polarity reversal occurs immediately after the receiver crosses the wire: $r_{SR} = a/2$. For model 2, the increase in the layer thickness is accompanied by an increase in r_{SR} (Fig. 4).

In both cases, the EMF in the central part of the loop reacts to changes of h_1, but practically does not depend on the offset. The closer the receiver is to the wire, whether outside or inside the loop, the faster the EMF changes with the receiver position.

The EMF in the center of the loop and r_{SR} react differently to a change in h_1. For a small (less than 2–3 m) layer thickness, r_{SR} weakly depends on h_1 (Fig. 7*a*). With further increase in the thickness of the layer, r_{SR} increases in direct proportion to h_1. In contrast to r_{SR}, the highest sensitivity of the EMF is observed in the range of h_1 from 2 to 10 m (Fig. 7*b*). For h_1 > 10 m, the increase in the layer thickness affects the EMF more and more weakly.

Obviously, both parameters can be used to determine the depth of a magnetically viscous base. As shown earlier, in studies of the magnetic viscosity effect on the transient responses of coaxial loop arrays (Kozhevnikov and Antonov 2009), the EMF in the center of the loop depends not only on h_1 but also on $\Delta\kappa_2$. Therefore, if h_1 is determined using the EMF at the center of the loop, measurements should be performed with *several* transmitter loops of *different* sizes which should be commensurable with h_1 (Kozhevnikov and Antonov, 2009, Figs. 5 and 6). This implies that for near-surface surveys, it is necessary to use small ($a \approx h_1$) transmitter loops. However, as seen in Fig. 4, when the layer is thin, a change in its thickness has a significant influence on the shape and level of profiling graphs, especially near the loop wire. Therefore, to determine h_1 and $\Delta\kappa_2$, we recommend an approach based on the measurements of EMF at several

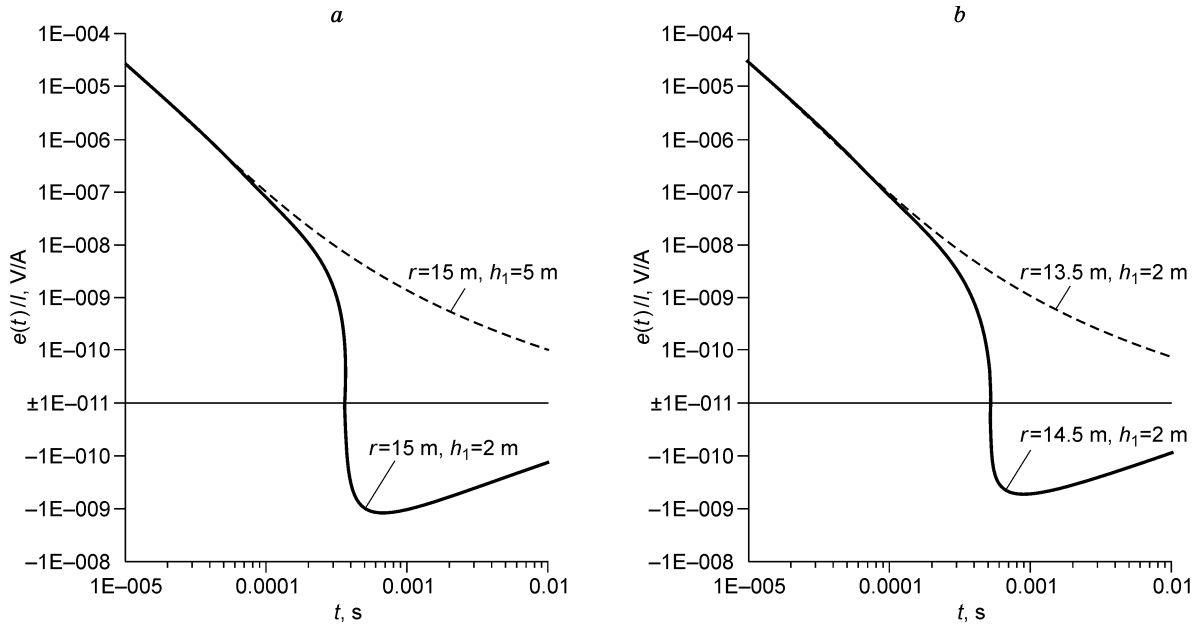

Fig. 6. Small changes in the depth to the top of the magnetic base (*a*) and in the offset (*b*) have a significant effect on the total transient response. The model parameters are $\rho_1 = \rho_2 = 10^2$ Ω·m, $\Delta\kappa_1 = 0$, and $\Delta\kappa_2 = 0.01$ SI units.

positions of the receiver near the side of a large ($a \gg h_1$) loop with the subsequent search for optimal parameters h_1 and $\Delta\kappa_2$. Unlike the EMF in the center of the loop, r_{SR} does not depend on $\Delta\kappa_2$. If r_{SR} is determined by profiling, h_1 can be immediately obtained using Fig. 7*b*. The discussion on the solution of the inverse problem by selecting model plots of the EMF remains valid for model 1 (Figs. 2 and 3). The proposed approach assumes that the effect of eddy currents can be neglected. Therefore, for its implementation, measurements should be performed at rather late times.

As shown above, the high sensitivity of the EMF to changes in r and h_1 is a favorable factor for determining the thickness of the layer. On the other hand, for a small layer thickness, the transient response reacts to small changes in r, so that minor errors in determining the position of the receiver will lead to large errors in model parameters.

At first glance, the magnetic viscosity effects may seem insignificant. Away from the wire and at a transmitter loop current of 1 A, the EMF induced in a receiver coil with an area of 1 m^2, is 10^{-10}–10^{-12} V (Figs. 2–5). However, in practical TEM surveys, the transmitter loop current is 10–100 A and the EMF is measured using inductive sensors with an effective area of 10^4–10^5 m^2 (Zakharkin, 1998). Therefore, the above estimate of the minimum EMF should be multiplied by 10^5–10^6, so that the range of EMF measured in the field

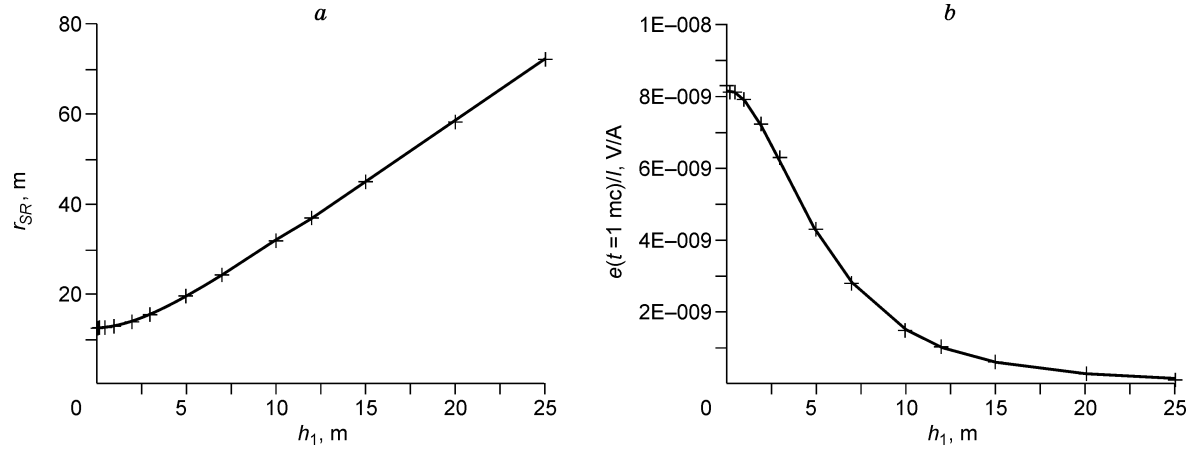

Fig. 7. Effect of the depth to the top of the magnetic base on r_{SR} (*a*) and EMF (t = 1 ms) in the center of the loop (*b*). The model parameters are $\rho_1 = \rho_2 = 10^6$ Ω·m, $\Delta\kappa_1 = 0$, and $\Delta\kappa_2 = 0.01$ SI units.

is 10^{-7}–10^{-4} V. Such EMF are typically measured in surveys using modern TEM systems.

Conclusions

1. Profiling graphs (the offset *r is* plotted on the abscissa, and the EMF induced in the receiver coil at a fixed time is plotted on the ordinate) show that the EMF polarity reverses as the offset increases. For the model with a magnetic layer, regardless of the layer thickness, polarity reversal occurs at small distance outside the loop. For the model with a magnetic base, the offset at which the EMF polarity reverses is the larger, the greater the thickness of the layer.

2. For both models, the EMF at a fixed time depends on the thickness of the layer and the offset. Particularly strong dependence of the EMF on layer thickness or offset is observed near the loop wire. Measurements in this area provide an opportunity to determine the thickness of the layer in the case where it is much smaller than the length of the loop side.

3. The overall effect of magnetic relaxation and transient eddy currents leads to the fact that for small changes in h_1 and r, the transient response changes dramatically.

4. Due to the fact that for a small layer thickness, the transient response reacts to small changes in *r,* a small error in the determination of the receiver position can lead to large errors in the estimated model parameters.

References

Buselli, G., 1982. The effect of near surface superparamagnetic material on electromagnetic transients. Geophysics 47 (9), 1315–1324.

Colani, C., Aitken, M.J., 1966. Utilization of magnetic viscosity effects in soils for archaeological prospecting. Nature, No. 5069, 1315–1324.

Heller, F., Evans, M.E., 2003. Environmental Magnetism: Principles and Applications of Enviromagnetics. Academic Press, New York.

Kozhevnikov, N.O. Antonov, E.Yu., 2008. The magnetic relaxation effect on TEM responses of a uniform earth. Russian Geology and Geophysics (Geologiya i Geofizika) 49 (3), 262–276 (197–205).

Kozhevnikov, N.O., Antonov, E.Yu., 2009. The magnetic relaxation effect on TEM responses of a two-layer earth. Russian Geology and Geophysics (Geologiya i Geofizika) 50 (10), 895–904 (1157–1170).

Kozhevnikov, N.O., Antonov, E.Yu., 2011. Magnetic relaxation of a horizontal layer: Effect on TEM data. Russian Geology and Geophysics (Geologiya i Geofizika) 52 (4), 398–404 (512–520).

Kozhevnikov, N.O., Antonov, E.Y., 2012. The TEM method in studies of near-surface magnetically viscous rocks, in: Near Surface Geoscience 2012—18th European Meeting of Environmental and Engineering Geophysics, 3–5 September 2012, Paris, France.

Kozhevnikov, N., Agafonov, Yu., Antonov, E., Buddo, I., Kompaniets, S., 2016. The effect of the Siberian flood basalts magnetic viscosity on a TEM sounding response. 23rd Electromagnetic Induction in the Earth Workshop, 14–20 August 2016, Chiang Mai, Thailand. S2.3-P272.

Lee, T.J., 1984. The transient electromagnetic response of a magnetic or superparamagnetic ground. Geophysics 49 (7), 854–860.

Linford, N., 2005. Archaeological applications of naturally occurring nanomagnets. J. Physics: Conference Series 17, 127–144.

Macnae, J., 2016. Quantitative estimation of intrinsic induced polarization and superparamagnetic parameters from airborne electromagnetic data. Geophysics 81 (6), E433–E446.

McNeill, J.D., 1980. Applications of Transient Electromagnetic Techniques: Technical Note TN-7. Geonics Limited, Mississauga, Ontario, Canada.

Stognii, V.V., Kozhevnikov, N.O., Antonov, E.Yu., 2010. TEM surveys for magnetic viscosity of rocks *in situ*. Russian Geology and Geophysics (Geologiya i Geophysika) 51 (11), 1219–1226 (1565–1575).

Worm, H.-U., Jackson, M., 1999. The superparamagnetism of Yucca Mountain Tuff. J. Geophys. Res. 104 (B11), 25,415–25,425.

Zakharkin, A.K., 1998. Compact receiver loop for TEM sounding. Rossiiskii Geofizicheskii Zh., No. 9–10, 95–99.

Zakharkin, A.K., Bubnov, V.M., Kryzhanovskii, V.A., Poletaeva, N.G., Tarlo, N.N., 1988. Magnetic viscosity of rocks as a new factor complicating TEM sounding, in: TEM Exploration for Minerals in Siberia [in Russian]. SNIIGGiMS, Novosibirsk, pp. 19–26.

Editorial responsibility: M.I. Epov